MPDU1 regulates CEACAM1 and cell adhesion in vitro and in vivo

Daniel C. Bennett[1], **Aurelie Cazet**[1], **Jon Charest**[1], and **Joseph N. Contessa**[1,2]

[1]Department of Therapeutic Radiology, Yale School of Medicine, New Haven 06510, Connecticut, USA

Abstract

N-linked glycosylation (NLG) is a co-translational modification that is essential for the folding, stability, and trafficking of transmembrane (TM) and secretory glycoproteins. Efficient NLG requires the stepwise synthesis and en bloc transfer of a 14-sugar carbohydrate known as a lipid-linked oligosaccharide (LLO). The genetics of LLO biosynthesis have been established in yeast and Chinese hamster systems, but human models of LLO biosynthesis are lacking. In this study we report that Kato III human gastric cancer cells represent a model of deficient LLO synthesis, possessing a homozygous deletion of the LLO biosynthesis factor, MPDU1. Kato III cells lacking MPDU1 have all the hallmarks of a glycosylation-deficient cell line, including altered sensitivity to lectins and the formation of truncated LLOs. Analysis of transcription using an expression microarray and protein levels using a proteome antibody array reveal changes in the expression of several membrane proteins, including the metalloprotease ADAM-15 and the cell adhesion molecule CEACAM1. Surprisingly, the restoration of MPDU1 expression in Kato III cells demonstrated a clear phenotype of increased cell-cell adhesion, a finding that was confirmed *in vivo* through analysis of tumor xenografts. These experiments also confirmed that protein levels of CEACAM-1, which functions in cell adhesion, is dependent on LLO biosynthesis in vivo. Kato III cells and the MPDU1-rescued Kato IIIM cells therefore provide a novel model to examine the consequences of defective LLO biosynthesis both *in vitro* and *in vivo*.

INTRODUCTION

N-linked glycosylation (NLG) is a conserved and essential protein modification that is critical for the function of endoplasmic reticulum (ER) translated glycoproteins. This co- and post- translational modification is especially important for transmembrane (TM) proteins, which typically contain multiple extracellular domain consensus sequons (NXS/T). NLG requires synthesis of glycan precursors, or lipid linked oligosaccharides (LLOs), of which the mature form contains fourteen carbohydrate subunits and is synthesized by at least eighteen enzymatic activities. In mammalian cells, efficient NLG contributes to proper folding, trafficking, and stability of TM and secretory proteins (Haga, Y., Ishii, K., et al. 2011)(Huang, P., Chen, C., et al. 2012).

[2]Corresponding Author: Joseph N. Contessa, Yale University School of Medicine, Department of Therapeutic Radiology, Smilow Cancer Hospital at Yale, New Haven, Connecticut 06510, Phone: 203-700-2634; Fax: 203-785-4622; joseph.contessa@yale.edu.

The steps of LLO biosynthesis are well understood due to a series of investigations in yeast and vertebrate NLG models (most of which are derived from hamster and mouse cell lines) where biochemical analysis has allowed a careful dissection of the LLO biosynthetic pathway (Jones, M.B., Tomiya, N., et al. 2010, Lehrman, M.A. and Zeng, Y. 1989, Patnaik, S.K. and Stanley, P. 2006, Stoll, J., Rosenwald, A.G., et al. 1988, Ware, F.E. and Lehrman, M.A. 1996). Additional genetic models are also available in other non-human vertebrates such as zebrafish (Cline, A., Gao, N., et al. 2012). Human cell models of NLG deficiency are limited to primary fibroblasts that have been collected from patients with congenital disorders of glycosylation (CDGs) (Rush, J.S., Panneerselvam, K., et al. 2000). CDG fibroblast models are useful, but frequently exhibit loss-of-function phenotypes rather than null phenotypes (Sun, L., Eklund, E.A., et al. 2005), which complicate *in vitro* phenotypic analyses.

Attempts to study NLG in tumors is also restricted by the lack of suitable models and cell lines. NLG is essential for the function of a number of TM proteins whose dysregulation has been implicated in human health, such as the receptor tyrosine kinases (RTKs) EGFR and Met. The RTKs are sensitive to tunicamycin, an inhibitor of NLG (Contessa, J.N., Bhojani, M.S., et al. 2008), and recent work has suggested that the inhibition of NLG may be sufficient to block RTK mediated resistance to radiation therapy (Contessa, J.N., Bhojani, M.S., et al. 2010). We recently established a model for the loss of mannose phosphate isomerase (MPI) using cancer cell lines stably expressing hairpin RNA constructs (Cazet, A., Charest, J., et al. 2014); this work allowed us to assess the effect of the loss of MPI on the function of individual RTKs. However, the effects of deficient NLG on the complement of TM and secretory glycoproteins in human cancer cells remain poorly understood.

In this study, we sought to identify and characterize human cancer cell models of NLG, with an emphasis on understanding the effects of the loss of NLG on TM glycoproteins. We report here the identification and initial characterization of a human gastric cancer cell line (Kato III) that is deficient in MPDU1, a key cofactor for dolichol-p-mannose transport into the ER and required for proficient LLO biosynthesis. Kato III cells lacking MPDU1 have corresponding defects in NLG and express a different membrane protein complement than rescued cells, several of which are implicated in cell adhesion. In order to examine the consequences of mature LLO deficiency in vivo, we also established xenograft tumors of Kato III cells and analyzed changes in molecular markers either with or without MPDU1 expression. Our results implicate MPDU1 as a mediator of glycoprotein stability and cell adhesion, providing a human model system for the investigation of NLG.

RESULTS

Kato III, a Human Gastric Adenocarcinoma Cell line is null for MPDU1

In our search for human model systems of defective N-linked glycosylation, we carried out an *in silico* screen of human cancer cell lines with copy number variations (CNVs) in enzymes responsible for the biosynthesis of lipid linked oligosaccharides (LLOs). Because the effect of a heterozygous loss or minor amplification may be difficult to predict, we focused on identifying cell lines bearing homozygous deletions in genes encoding LLO biosynthesis factors. We were surprised to find that, despite the marked genomic instability

that is a hallmark of cancer cells, cell lines with deletions in LLO synthesis genes are exceedingly rare; only one cell line in the COSMIC database (Kato III) contains a homozygous deletion of a gene required for mature LLO synthesis (MPDU1; Table 1). MPDU1 is required for the availability of Man-p-dolichol and Glc-p-dolichol in the lumen of the endoplasmic reticulum, and a loss of MPDU1 function results in truncated LLOs (Ware, F.E. and Lehrman, M.A. 1996)(Schenk, B., Imbach, T., et al. 2001). In Kato III cells, the gene deletion removes the entire coding region of MPDU1 along with neighboring genes including TP53.

We verified the presence of a homozygous MPDU1 deletion in Kato III genomic DNA by PCR (Fig. 1A). PCR failed to amplify a PCR product from exons 2-3 of MPDU1 in Kato III cells, but amplified MPDU1 from a control D54 glioma cell line, confirming the loss of MPDU1 in Kato cells. PCR amplification of exon 10 of ALG6, a second gene required for mature LLO synthesis, was also carried out as a positive control. To investigate the consequences of MPDU1 loss in the Kato III cell line, we generated stable clones transfected with a full-length cDNA encoding MPDU1 (Kato IIIM1-3) (Fig. 1B). Loss of MPDU1 in CHO cells is known to enhance toxicity to lectin treatment in the context of mannosidase inhibition with swainsonine. In CHO cells loss of MPDU1 increases sensitivity to swainsonine plus Concanavalin A (ConA) but also reduces sensitivity to swainsonine plus phytohemagglutinin (PHA). We therefore analyzed the sensitivity of Kato III cells to cytotoxic lectins as an indirect measurement of their surface glycoprotein composition (Ware, F.E. and Lehrman, M.A. 1996). Restoring MPDU1 increased the sensitivity of Kato III cells to concanavalin A in the presence of swainsonine and decreased the sensitivity of Kato III cells to phytohemagglutinin in the presence of swainsonine (Fig. 1C). These results suggest that MPDU1 transfected Kato III cells changed cell surface glycans from a predominantly high mannose type to a complex glycan type, an observation consistent with rescue of mature LLO biosynthesis. To directly evaluate whether the re-expression of MDPU1 in Kato III cells corrects a defect in LLO biosynthesis, we performed fluorophore-assisted carbohydrate electrophoresis (FACE) analysis of LLOs in Kato III and MPDU1-rescued cells. Our results show that LLOs in Kato III cells are truncated and correspond to the Man5GlcNac2 species and that the expression of MPDU1 rescues the synthesis of the mature LLO (Fig. 1D). This data unequivocally confirms the biosynthetic defect in LLO synthesis in Kato III cells and demonstrates the ability to rescue this defect with re-expression of MPDU1. Kato III cells and Kato III cells with MPDU1 expression (hereafter referred to as Kato IIIM) therefore represent a novel human cell line pair that can be used to study the consequences of defective LLO biosynthesis.

The selective pressures and adaptations of Kato III tumor cells to survive MPDU1 loss are unknown. We investigated the effects of MPDU1 on the epidermal growth factor receptor (EGFR), a receptor tyrosine kinase known to drive tumor cell proliferation and whose activation can be blocked by aberrant glycosylation. Western blots for EGFR demonstrated no change in receptor levels between Kato III and Kato IIIM, though a size increase was observed in Kato IIIM consistent with improved glycosylation (Fig. 2A). We compared these results to those from Lec35 CHO cells, which are also MPDU1 defective, after stable transfection of an EGFR-GFP. These experiments demonstrated that individual Lec35 clones have variable phenotypes with respect to EGFR expression (Fig. 2B). Using microscopy we

observed clones with either a predominant cytoplasmic GFP signal (clone 1) or a with localization to the secretory compartment (clone 2). Western blots of these clones after treatment with or without the proteasome inhibitor, bortezomib, demonstrated that EGFR was actively degraded in clone 1 (consistent with the cytoplasmic GFP signal) whereas clone 2 had adapted to express abnormally glycosylated EGFR at high levels (Fig. 2C). The results from Lec35 cells suggest that the Kato cell line has adapted to maintain expression levels of important glycoproteins.

MPDU1 affects the transcription of membrane and ER genes in Kato III cells

The Kato III cell lines are the first human model system bearing a homozygous null deletion of a gene required for LLO biosynthesis. The complete loss of MPDU1, in contrast to partial loss of function observed from patients with this congenital disorders of glycosylation (CDG-IF; Kranz C, Denecke J et. al. 2001), provides an opportunity to more clearly delineate the differences between cells that are proficient or deficient in LLO biosynthesis. We first examined the transcriptional profiles of Kato III and Kato III-M cells to examine the presence or absence of a transcriptional response to re-expression of MPDU1. We carried out expression microarray analysis comparing the global mRNA levels of Kato III cells to Kato IIIM and mapped the gene ontology (GO) terms for the differentially expressed genes (Fig. 3A). MPDU1 was the most up-regulated gene in Kato III-M cells (data not shown), confirming that MPDU1 was restored and that the samples differed with respect to MPDU1 status. Furthermore, TP53 and other factors involved in LLO biosynthesis (e.g., the ALG genes and DOLK) showed no changes after MPDU1 rescue. Surprisingly these experiments revealed a distinct set of differentially expressed genes that were assigned to a small number of specific gene ontologies. The most overrepresented GO terms ($p < 0.001$) were those corresponding to biological membranes (plasma membrane, GO), the endoplasmic reticulum, and the endomembrane system in general. These results show that the re-expression of MPDU1 activates an alternative transcriptional program that regulates the transcription of ER and plasma membrane proteins.

MPDU1 Regulates levels of cell surface glycoproteins

The major advantage for identifying a human model system with defects in the LLO biosynthetic system is the accessibility of tools to analyze changes in protein expression. Although several rodent cell lines with defects in either MPDU1, DPM1/2, or ALG6 have been described ((Ware, F.E. and Lehrman, M.A. 1996)(Maeda, Y., Tomita, S., et al. 1998) (Chapman, A., Fujimoto, K., et al. 1980)), the species origin of these models significantly complicates analyses such as protein profiling. To demonstrate the utility of the Kato cell line model, we examined changes in protein expression using a commercially available receptor protein array (Fig. 4A). The analysis of protein levels using this approach showed that 6 glycoproteins (CEACAM-1, CEACAM-5, ADAM-15, TIMP-1, Nestin-2, and Integrin B5) were expressed at higher levels in the setting of MPDU1 expression. CEACAM-1 and ADAM-15 had the highest differential expression in the protein array screen and were therefore tested by western blot analysis. Results from these experiments in multiple MPDU1-expressing clones confirmed that CEACAM-1 and ADAM-15 levels are associated with MPDU1 expression (Fig. 4B). Together, these data show that rescuing a defect in LLO biosynthesis can have effects on the levels of specific glycoproteins.

MPDU1 Regulates cell adhesion and CEACAM1 expression in vivo

The final advantage of the Kato III model is the ability to grow these cell lines as xenograft tumors in immune-deficient mice. This characteristic provides an experimental approach to determine whether *in vitro* observations are also reproduced during the more complex three dimensional growth of tissues. We therefore tested the validity of two *in vitro* findings in Kato xenograft tumors. First, during generation of the Kato IIIM clones we observed a distinctive growth pattern in clones expressing MPDU1. While Kato III wild type cells grow as a semi-adherent culture, Kato IIIM cells displayed increased cell-cell adhesion under normal culture conditions (Fig. 5A). This growth pattern became an effective surrogate for identifying MPDU1 expression, as all five confirmed sub-clones displayed this growth pattern.

To quantify this difference we took advantage of the semi-adherent growth pattern of Kato cells. In short term cultures 48 hrs after trypsinization the size of floating cell aggregates were quantified. A count of non-adherent cells treated with trypsin showed that 97% of Kato III and and 96% of Kato IIIM cells have a size 10 microns, consistent with single cells. In contrast counts of the identical cell cultures without trypsin treatment showed a significant increase in the size of cell aggregates (~10% of all cells) for Kato IIIM (Fig. 5B, p <.01). This data demonstrates increased cell-cell aggregation for Kato IIIM even at short term periods after recovery from trypsinization.

We next examined whether Kato xenografts also display different growth patterns. Representative hematoxylin and eosin stains of Kato xenografts (Fig. 6, top) shows that Kato III tumors grow as poorly organized sheets of cells, but that Kato IIIM xenografts grow in a more organized and glandular pattern. We interpret these *in vitro* and *in vivo* findings to represent a change in glandular structure organization *via* cell-cell adhesion caused by rescue of the LLO biosynthetic defect.

We also explored the ability of our *in vitro* protein screening arrays to predict the state of *in vivo* protein levels, and examined CEACAM1 protein levels in both Kato III and Kato IIIM xenografts using IHC. Our results demonstrate that MPDU1 rescue also increases cytoplasmic CEACAM1 expression in vivo (Fig. 6). This result is consistent with a positive IHC control for MPDU1 and a negative IHC control for calnexin that show increased or unchanged *in vivo* expression respectively.

DISCUSSION

This report characterizes the first human cell line with a homozygous defect in a gene required for LLO biosynthesis. This cancer cell line was identified through the COSMIC database and presents a unique opportunity to investigate the consequences of an LLO synthesis defect. The lack of other LLO synthesis-deficient cancer cell lines, despite the marked genomic instability of cancer cells, is significant. There are over 1000 cell lines with sequencing information in the COSMIC database but only the Kato III cells are reported to have acquired this defect. We believe the rarity of this biosynthetic defect in this population of cell lines indicates that complete loss of mature LLO biosynthesis and abnormal N-linked glycosylation is not well-tolerated by cancer cells. This interpretation supports a model

where NLG is fundamentally important for tumorigenesis and tumor progression, and provides evidence to suggest N-linked glycosylation may be a promising clinical target in cancer (Contessa, J.N., Bhojani, M.S., et al. 2010).

The Kato III cell line was isolated from a malignant pleural effusion of a 55 year old Japanese male with gastric adenocarcinoma (Sekiguchi M, Sakakibara K, et. al. 1978). Consistent with this metastatic anatomic site, the resultant tumor cells are poorly differentiated and capable of semi-adherent growth. This cell line's loss of adhesion has been attributed, in part, to a heterozygous mutation of E-Cadherin (Karam R, Carvalho J et. al. Oncogene 2008), a tumor suppressor protein frequently mutated in malignant gastrointestinal tumors. However, our rescue experiments with MPDU1 both *in vitro* and *in vivo* suggest that the observed loss in cell-cell adhesion is also dependent on MPDU1 and mature LLO biosynthesis. Because CHO Lec35 cells (which are also null for mpdu1) do not display an adhesion deficit, the co-existing deficit in E-cadherin function could be responsible for revealing the adhesion phenotype difference. However, considering the known clinical GI manifestation of protein losing enteropathy and hepatic fibrosis in patients with CDG (Liem, Y.S., Bode, L., et al. 2008), it is also possible that gastrointestinal cell differentiation could underlie the observed cell-cell adhesion defect mediated by MPDU1. In either case, our work using the Kato III cell line supports a model where specific phenotypes caused by incomplete LLO synthesis are revealed by genetic or epigenetic interactions in the affected cell or tissue.

The identification of a human cell line with an LLO deficit provides a new opportunity to profile changes in cellular biology using array formats. In this work, we report differences in both mRNA and protein expression using the Kato III and Kato IIIM cell lines. The mRNA microarray results demonstrate induction of specific transcriptional programs that regulate membrane proteins, and provide potential biomarkers for evaluating and understanding changes that occur in the setting of LLO defects. We have also identified glycoprotein biomarkers of defective LLO synthesis with this model system. Using a protein array as a screen and western blot for validation, we identified enhanced protein levels of several glycoproteins after MPDU1 rescue. The transmembrane glycoprotein CEACAM-1 was found to have the most striking change in this system with nearly undetectable levels in Kato cells and high expression after MPDU1 rescue. This protein has 20 N-linked glycosylation sites that contribute up to half of the glycoprotein's final molecular weight (Lucka, L., Fernando, M., et al. 2005) and therefore it is not surprising that CEACAM1 protein levels could be a marker for aberrant LLO biosynthesis. CEACAM1 is a known cell adhesion molecule that contributes to cell-cell adhesion through homophilic interactions (Benchimol, S., Fuks, A., et al. 1989, Obrink, B. 1997) and thus is likely a contributor to the adhesion phenotype observed in this model system. It is of interest that CEACAM-1 also mediates interactions with pathogenic bacteria of the GI tract (Baranov, V. and Hammarstrom, S. 2004, Chorny, A. and Cerutti, A. 2012), and thus it is tempting to speculate that reduced LLO biosynthesis could also affect other diverse cellular or environmental interactions.

Although Kato III cell lines are the first human model system that provides a clear cellular phenotype for defects in LLO biosynthesis, an inherent limitation of this work is that our findings may not be representative of non-transformed and non-tumorigenic cells. Cancer

cells and cells undergoing normal development do, however, share many properties including increased metabolic demands and initiation of cell surface receptor dependent programs such as proliferation, migration, invasion, and cell survival. In patients, defects in LLO biosynthesis and N-linked glycosylation have significant consequences for developing tissues, and thus tumor models like the Kato cells may provide an additional (though imperfect) approach for studying the consequences of defective LLO biosynthesis. In support of this idea, we have also recently identified altered FGFR signaling in glioma cell lines with knockdown of MPI function (Cazet, A., Charest, J., et al. 2014). Together our work using these transformed cell lines suggest that tumor models may better tolerate defects in LLO biosynthesis and therefore allow investigations into cellular outcomes of dysfunctional N-linked glycosylation.

Finally a noteworthy characteristic of the Kato cell lines is their ability to grow both *in vitro* as a cell culture and *in vivo* as xenograft tumors. This is an important feature of any model system because it allows for the exclusion of findings that are the product of an *in vitro* artifact. Kato xenografts provide an opportunity to study LLO deficits under conditions that reflect more complex cellular growth patterns reliant upon physiological constraints. In our study we demonstrate that our *in vitro* findings of increased cellular organization and enhanced expression of specific proteins (e.g., CEACAM1) also occur *in vivo*. Kato III cell lines therefore provide a valuable model for the study of defective LLO synthesis and aberrant N-linked glycosylation.

In summary, we have characterized an MPDU1 null human cell line to demonstrate the role of this protein in regulating levels of glycoproteins like CEACAM1 as well as in mediating cell adhesion. We believe that the Kato III cell line and its MPDU1 rescued counterpart, Kato IIIM, will provide a novel and useful model system to study the cellular consequences of defects in LLO biosynthesis.

Materials and Methods

Antibodies and reagents

The mouse monoclonal anti-β-actin (Catalog #8H10D10) and anti-E-cadherin antibodies were purchased from Cell Signaling Technology, Inc. (Danvers, MA, USA). The anti-MPDU1 antibody was purchased from Sigma-Aldrich (St. Louis, MO, USA). The anti-human CEACAM-1 antibody (Catalog #MAB2244) was purchased from R&D Systems® (Minneapolis, MN, USA).

Cell Culture

Cell culture reagents were purchased from Gibco (Grand Island, NY, USA). The human gastric carcinoma cell line Kato III (ATCC #HTB-103) was obtained from the American Type Culture Collection (Rockville, MD, USA). Kato III cells were grown in RPMI-1640 medium supplemented with 10% fetal bovine serum (FBS) and 100 units/mL penicillin-streptomycin as semi-adherent cultures and maintained at 37°C in a humidified 5% CO_2 atmosphere. Cell counting was perfomed with a Z2 Coulter Counter and size cutoffs for quantification set at 10, 10-20, or 20-30 microns. The Lec35 cell line was a gift from Mark

Lehrman (UT Southwestern, Dallas Tx) and stable transfection of the EGFR-GFP was performed as previously described (Contessa, J.N., Bhojani, M.S., et al. 2008).

PCR Amplification of MPDU1

Exons 2 and 3 of MPDU1 were amplified from genomic DNA using Taq polymerase (Invitrogen, Carlsbad, CA, USA) and the primers MDPU1-23F (5′ - CCCTGCCTCAAGATTCTCCTC - 3′) and MPDU1-23R (5′- GGGAAGTTGTTAGTGATGCTGTAGA - 3′) using a standard PCR program of 94°C - 4 min, 30 cycles of 94°C – 30 sec, 55°C – 30 sec, 72°C 30 sec, 72° for 7 min in a thermal cycler (MJ Research/Bio-Rad, Hercules, CA, USA). The PCR products were visualized by agarose gel electrophoresis with ethidium bromide; MPDU1 was scored by the presence or absence of a 191-base pair band. ALG6 was amplified as a control from genomic DNA using the primers ALG6-FA (5′-TCAGATAATCAATGTTTGTGAAATGAGG - 3′) and ALG6-RA (5′- GATCAGTTGTGGCAAGAATTAAGTATC -3′).

MPDU1 rescue and stable transfection of Kato III cells

A cDNA encoding full-length human MPDU1 was obtained from OriGene (Rockville, MD, USA) and transfected into Kato III cells using Lipofectamine 2000 (Invitrogen) according to the manufacturer's instructions. Twenty-four hours after transfection, G418 (Gibco) was added to a final concentration of 400 ng/mL, and the cells were incubated for 72h at 37°C in a humidified 5% CO_2 atmosphere. Individual G418-resistant colonies were isolated by limiting dilution into 96-well plates and sequentially expanded to 12-well plates. Three positive clones that expressed high levels of MPDU1 as determined by PCR and Western blot analysis were selected for further study.

Fluorophore-assisted Carbohydrate Electrophoresis (FACE)

Lipid-linked oligosaccharides were extracted essentially as described (Gao, N. and Lehrman, M.A. 2002), (Hori, H. and Elbein, A.D. 1982). Briefly, for the semi-adherent Kato-III cells, the adherent cells were removed by scraping, and the floating and adherent cells were pooled and centrifuged at $500 \times g$ for 5 minutes. The cell pellet was washed twice with 4° C PBS and then resuspended in 1 mL of 4° C methanol. The methanol suspension was evaporated to near-dryness under a vacuum using a SpeedVac (ThermoFisher Savant SC100, Waltham, MA, USA) modified to accept 15-mL centrifuge tubes. The near-dry pellet was resuspended in 0.9 mL of water and sonicated for 2 minutes with one-second on-off pulses. One and a half milliliters of methanol was added to the aqueous cell suspension, and this mixture was vortexed for 30 seconds and then sonicated. Three milliliters of chloroform was added to this mixture, and the tubes were vortexed for 1 minute. The reactions were centrifuged at $3000 \times g$ for 10 minutes to resolve three phases, and the middle LLO-containing pellet was retained. This pellet was resuspended in 3 mL of a freshly-prepared mixture of chloroform, methanol and water (10:10:3); this suspension was spun at $3000 \times g$ for 10 minutes, and the entire solute was retained and dried completely under vacuum. The LLOs were extracted from this pellet by mild acid hydrolysis; the pellet was resuspended in 80% tetrahyrdofuran, and then 37% hydrochloric acid was added to a final concentration of 0.1 M and the tubes placed in a 50° C water bath for 90 minutes. After hydrolysis, the THF/HCl mixture was dried completely under a vacuum, the pellet was resuspended in 400

μL of water, and 1 mL of a freshly-prepared mixture of chloroform and methanol (2:1) was added. This suspension was vortexed and spun at $3000 \times g$ for 10 minutes to resolve two phases; the aqueous phase was dried under a vacuum for labeling and gel analysis. LLOs were labeled with 8-aminonaphthalene-1,3,6-trisulfonic acid (ANTS) using a commercially available labeling kit according to the manufacturer's protocol (Prozyme, Hayward, CA, USA), resolved by electrophoresis through oligosaccharide profiling gels (Prozyme), and observed using a UV gel documentation system (Syngene G:BOX, Frederick, MD, USA) fitted with a digital camera and a 302/365nm UV converter plate (VWR, Irving, TX, USA).

Lectin Selection Assays

For lectin selection, 1×10^3 cells were plated in 96-well plates and incubated overnight. The following day, Swainsonine (2 μg/mL, EMD Calbiochem, Philadelphia, PA, USA) and either Concanavalin A (12.5 μg/mL, EMD Calbiochem) or Erythroagglutinin (40 μg/mL, Sigma-Aldrich) were added,, and the plates were incubated for 72 hours. After 72h, the surviving cells were assayed by tetrazolium reduction (MTS) according to the manufacturer's protocol (Promega, Madison, WI, USA), the absorbance was read using a multiplate reader (BioTek Synergy HT, Winooski, VT, USA), and the data were normalized swainsonine treated controls.

Immunoblotting

G418-resistant Kato III clones were resuspended in lysis buffer (25 mM Tris-HCl pH 7.4, 10 mM EDTA, 15% glycerol, 0.1% Triton X-100, protease inhibitor tablet (Roche Diagnostics; Indianapolis, IN, USA), and phosphatase inhibitor cocktails 2 and 3 (Sigma-Aldrich, St. Louis, MO, USA)). The protein concentration of supernatants was assessed using the Bio-Rad *RC* protein assay kit II (Bio-Rad, Hercules, CA, USA). Twenty micrograms of total protein from each cell lysate was subjected to SDS-PAGE and transferred onto a PDVF membrane (Millipore). The membranes were saturated in TBS-0.05% Tween® 20 (TBST, Sigma-Aldrich) containing either 5% (w/v) nonfat dry milk (American Bioanalytical; Natick, MA, USA) or 5% bovine serum albumin (Sigma-Aldrich). The membranes were then incubated overnight at 4°C with the primary antibody, thoroughly washed with TSBT, and incubated at room temperature for 1 hour - with a horseradish peroxidase-conjugated anti-rabbit or anti-mouse secondary antibody. Immunoreactive bands were visualized by chemiluminescence using the Western Lightning® *Plus*-ECL reagent (PerkinElmer; Waltham, MA, USA) and Kodak film (Sigma-Aldrich).

Analysis of human soluble receptors and related proteins

The Kato III control cells and MPDU1-positive clones were cultured normally in serum-containing medium. The cells were pelleted and rinsed several times in cold phosphate-buffered saline (PBS). The non-hematopoietic Proteome Profiler Human sReceptor Array kit (R&D Systems) was used to measure the protein levels of human soluble receptors according to the manufacturer's protocol. Briefly, Kato cells were lysed in kit-supplied Lysis Buffer 15 supplemented with a protease inhibitor tablet (Roche Diagnostics). The protein concentrations of the supernatants were assessed using the Bio-Rad *RC* protein assay kit II (Bio-Rad). The N and C arrays were then blocked in the appropriate blocking buffer for one hour and incubated overnight at 4° C with 200 μg of total protein extract. The N and C

arrays were washed three times and incubated with the appropriate horseradish peroxidase-conjugated N or C detection antibody cocktail for 2 hours at room temperature and then treated with Western Lightning® *Plus*-ECL reagent (Perkin Elmer) and exposed to Kodak autoradiography film.

Microarray analysis

For microarray analysis, Kato III cells and MPDU1-positive Kato III clones were grown in standard growth medium in triplicate 10-cm dishes. Approximately 1×10^7 cells were removed from each plate by washing and scraping and centrifuged at $500 \times g$ for 5 minutes. Total RNA was isolated from the cells using TRIzol reagent (Sigma) according to the manufacturer's protocol. The extracted total RNA was purified using the RNEasy MinElute cleanup kit (QIAgen, Hilden, Germany) according to the manufacturer's protocol. The purity of the resulting eluate was determined by measuring the A260/A280 ratio using a NanoDrop spectrophotometer (NanoDrop/Thermo Scientific); all samples had 260/280 ratios of at least 1.8. The purified RNA samples were further processed by the Yale Center for Genome Analysis; first-strand cDNA was synthesized for each sample and then hybridized in triplicate to Affymetrix Human Gene 1.0 ST arrays (Catalog #901086; Affymetrix, Inc., Santa Clara, CA, USA). The samples from the Kato III cells were compared to those from the MPDU1-positive Kato III clones. The microarray data were scanned by the YCGA and analyzed at the gene level using Genespring GX version 12 (Agilent Technologies, Santa Clara, CA, USA). Genes with fold changes greater than 2.0 at an FDR-adjusted p-value of less than 0.05 were selected for further analysis. The gene ontology (GO) terms for these differentially expressed genes were collated and sorted by frequency.

Mouse xenografts and immunohistochemistry

Kato III cells and MPDU-1-positive Kato III clones were grown under normal conditions in 15-cm dishes. The cells were harvested by both trypsination of adherent and collection of non-adherent cells by centrifugation. Approximately 10×10^6 cells were injected injected subcutaneously into the flanks of NOD-SCID mice. Tumors were allowed to grow for a period of ~ 3 weeks. When palpable tumors were detected, the mice were sacrificed and excised xenografts were formalin fixed, dehydrated in ethanol, and paraffin embedded for immunohistochemistry (IHC). Sections were stained with standard hematoxilin and eosin or with the indicated primary antibody. A secondary HRP-conjugated antibody and DAB was used to resolve the antigen signal.

Acknowledgments

Abbreviations

LLO	lipid-linked oligosaccharide

NLG	N-linked glycosylation
ER	endoplasmic reticulum
CHO	Chinese hamster ovary
CDG	congenital disorder of glycosylation
MPDU	mannose-P-dolichol utilization
Man	mannose
GlcNac	N-acetylglucosamine
FACE	fluorophore-assisted carbohydrate electrophoresis
CNV	copy number variation
H&E	hematoxylin and eosin
PBS	phosphate-buffered sailne

References

Anand M, Rush JS, Ray S, Doucey MA, Weik J, Ware FE, Hofsteenge J, Waechter CJ, Lehrman MA. Requirement of the Lec35 gene for all known classes of monosaccharide-P-dolichol-dependent glycosyltransferase reactions in mammals. Molecular biology of the cell. 2001; 12:487–501. [PubMed: 11179430]

Baranov V, Hammarstrom S. Carcinoembryonic antigen (CEA) and CEA-related cell adhesion molecule 1 (CEACAM1), apically expressed on human colonic M cells, are potential receptors for microbial adhesion. Histochemistry and cell biology. 2004; 121:83–89. [PubMed: 14758482]

Benchimol S, Fuks A, Jothy S, Beauchemin N, Shirota K, Stanners CP. Carcinoembryonic antigen, a human tumor marker, functions as an intercellular adhesion molecule. Cell. 1989; 57:327–334. [PubMed: 2702691]

Cazet A, Charest J, Bennett DC, Sambrooks CL, Contessa JN. Mannose phosphate isomerase regulates fibroblast growth factor receptor family signaling and glioma radiosensitivity. PloS one. 2014; 9:e110345. [PubMed: 25314669]

Chapman A, Fujimoto K, Kornfeld S. The primary glycosylation defect in class E Thy-1-negative mutant mouse lymphoma cells is an inability to synthesize dolichol-P-mannose. The Journal of biological chemistry. 1980; 255:4441–4446. [PubMed: 7372584]

Chorny A, Cerutti A. CEACAM1-S: the virtues of alternative splicing in gut immunity. Immunity. 2012; 37:768–770. [PubMed: 23159224]

Cline A, Gao N, Flanagan-Steet H, Sharma V, Rosa S, Sonon R, Azadi P, Sadler KC, Freeze HH, Lehrman MA, et al. A zebrafish model of PMM2-CDG reveals altered neurogenesis and a substrate-accumulation mechanism for N-linked glycosylation deficiency. Molecular biology of the cell. 2012; 23:4175–4187. [PubMed: 22956764]

Contessa JN, Bhojani MS, Freeze HH, Rehemtulla A, Lawrence TS. Inhibition of N-linked glycosylation disrupts receptor tyrosine kinase signaling in tumor cells. Cancer research. 2008; 68:3803–3809. [PubMed: 18483264]

Contessa JN, Bhojani MS, Freeze HH, Ross BD, Rehemtulla A, Lawrence TS. Molecular imaging of N-linked glycosylation suggests glycan biosynthesis is a novel target for cancer therapy. Clinical cancer research : an official journal of the American Association for Cancer Research. 2010; 16:3205–3214. [PubMed: 20413434]

Gao N, Lehrman MA. Analyses of dolichol pyrophosphate-linked oligosaccharides in cell cultures and tissues by fluorophore-assisted carbohydrate electrophoresis. Glycobiology. 2002; 12:353–360. [PubMed: 12070078]

Haga Y, Ishii K, Suzuki T. N-glycosylation is critical for the stability and intracellular trafficking of glucose transporter GLUT4. The Journal of biological chemistry. 2011; 286:31320–31327. [PubMed: 21757715]

Hori H, Elbein AD. Characterization of the oligosaccharides from lipid-linked oligosaccharides of mung bean seedlings. Plant physiology. 1982; 70:12–20. [PubMed: 16662430]

Huang P, Chen C, Mague SD, Blendy JA, Liu-Chen LY. A common single nucleotide polymorphism A118G of the mu opioid receptor alters its N-glycosylation and protein stability. The Biochemical journal. 2012; 441:379–386. [PubMed: 21864297]

Jones MB, Tomiya N, Betenbaugh MJ, Krag SS. Analysis and metabolic engineering of lipid-linked oligosaccharides in glycosylation-deficient CHO cells. Biochemical and biophysical research communications. 2010; 395:36–41. [PubMed: 20331963]

Karam R, Carvalho J, Bruno I, Graziadio C, Senz J, Huntsman D, Carneiro F, Seruca R, Wilkinson MF, Oliveira C. The NMD mRNA surveillance pathway downregulates aberrant E-cadherin transcripts in gastric cancer cells and in CDH1 mutation carriers. Oncogene. 2008; 27:4255–60. 2008. [PubMed: 18427545]

Kranz C, Denecke J, Lehrman MA, Ray S, Kienz P, Kreissel G, Sagi D, Peter-Katalinic J, Freeze HH, Schmid T, Jackowski-Dohrmann S, Harms E, Marquardt T. A mutation in the human MPDU1 gene causes congenital disorder of glycosylation type If (CDG-If). J Clin Invest. 2001; 108:1613–9. [PubMed: 11733556]

Lehrman MA, Zeng Y. Pleiotropic resistance to glycoprotein processing inhibitors in Chinese hamster ovary cells. The role of a novel mutation in the asparagine-linked glycosylation pathway. The Journal of biological chemistry. 1989; 264:1584–1593. [PubMed: 2521484]

Liem YS, Bode L, Freeze HH, Leebeek FW, Zandbergen AA, Paul Wilson J. Using heparin therapy to reverse protein-losing enteropathy in a patient with CDG-Ib. Nature clinical practice. Gastroenterology & hepatology. 2008; 5:220–224. [PubMed: 18285818]

Lucka L, Fernando M, Grunow D, Kannicht C, Horst AK, Nollau P, Wagener C. Identification of Lewis x structures of the cell adhesion molecule CEACAM1 from human granulocytes. Glycobiology. 2005; 15:87–100. [PubMed: 15317738]

Maeda Y, Tomita S, Watanabe R, Ohishi K, Kinoshita T. DPM2 regulates biosynthesis of dolichol phosphate-mannose in mammalian cells: correct subcellular localization and stabilization of DPM1, and binding of dolichol phosphate. The EMBO journal. 1998; 17:4920–4929. [PubMed: 9724629]

Obrink B. CEA adhesion molecules: multifunctional proteins with signal-regulatory properties. Curr Opin Cell Biol. 1997; 9:616–626. [PubMed: 9330864]

Patnaik SK, Stanley P. Lectin-resistant CHO glycosylation mutants. Methods in enzymology. 2006; 416:159–182. [PubMed: 17113866]

Rush JS, Panneerselvam K, Waechter CJ, Freeze HH. Mannose supplementation corrects GDP-mannose deficiency in cultured fibroblasts from some patients with Congenital Disorders of Glycosylation (CDG). Glycobiology. 2000; 10:829–835. [PubMed: 10929009]

Schenk B, Imbach T, Frank CG, Grubenmann CE, Raymond GV, Hurvitz H, Korn-Lubetzki I, Revel-Vik S, Raas-Rotschild A, Luder AS, et al. MPDU1 mutations underlie a novel human congenital disorder of glycosylation, designated type If. The Journal of clinical investigation. 2001; 108:1687–1695. [PubMed: 11733564]

Sekiguchi M, Sakakibara K, Fujii G. Establishment of cultured cell lines derived from a human gastric carcinoma. Jpn J Exp Med. 1978; 48:61–8. [PubMed: 209229]

Stoll J, Rosenwald AG, Krag SS. A Chinese hamster ovary cell mutant F2A8 utilizes polyprenol rather than dolichol for its lipid-dependent asparagine-linked glycosylation reactions. The Journal of biological chemistry. 1988; 263:10774–10782. [PubMed: 3392042]

Sun L, Eklund EA, Van Hove JL, Freeze HH, Thomas JA. Clinical and molecular characterization of the first adult congenital disorder of glycosylation (CDG) type Ic patient. American journal of medical genetics. Part A. 2005; 137:22–26. [PubMed: 16007612]
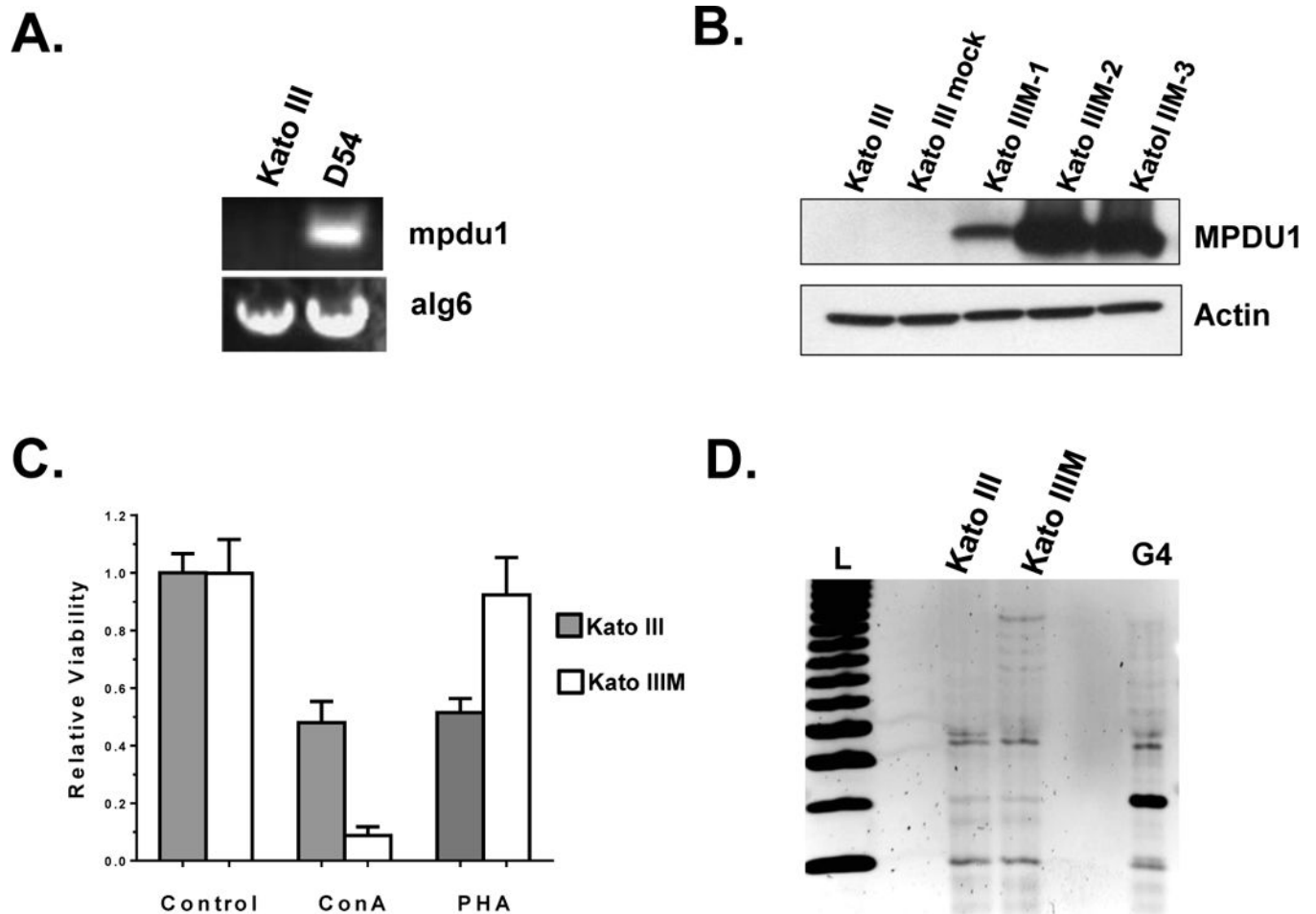
Ware FE, Lehrman MA. Expression cloning of a novel suppressor of the Lec15 and Lec35 glycosylation mutations of Chinese hamster ovary cells. J Biol Chem. 1996; 271:13935–13938. [PubMed: 8663248]

Figure 1. Kato III cells lack MPDU1 activity and have abnormal NLG

(A) PCR for mpdu1 or alg6 from kato III or D54 tumor cell lines. **(B)** Western blot of Kato III cells, mock transfected cells, and three independent MPDU1-transfected Kato III clones (Kato IIIM1-3). Actin was used as a loading control. **(C)** Lectin toxicity in Kato III and Kato IIIM cells measured by MTT. All cells were swainsonine treated with or without the addition of concanavalin A (ConA) or Erythroagglutinin (PHA-E). **(D)** Fluorophore-assisted carbohydrate electrophoresis (FACE) in Kato III and Kato IIIM cells demonstrating accumulation and rescue of DolP-Man5-GlcNac2 LLO intermediates. Columns 1 and 4 show the glycan ladder and tetraglucose controls, respectively.
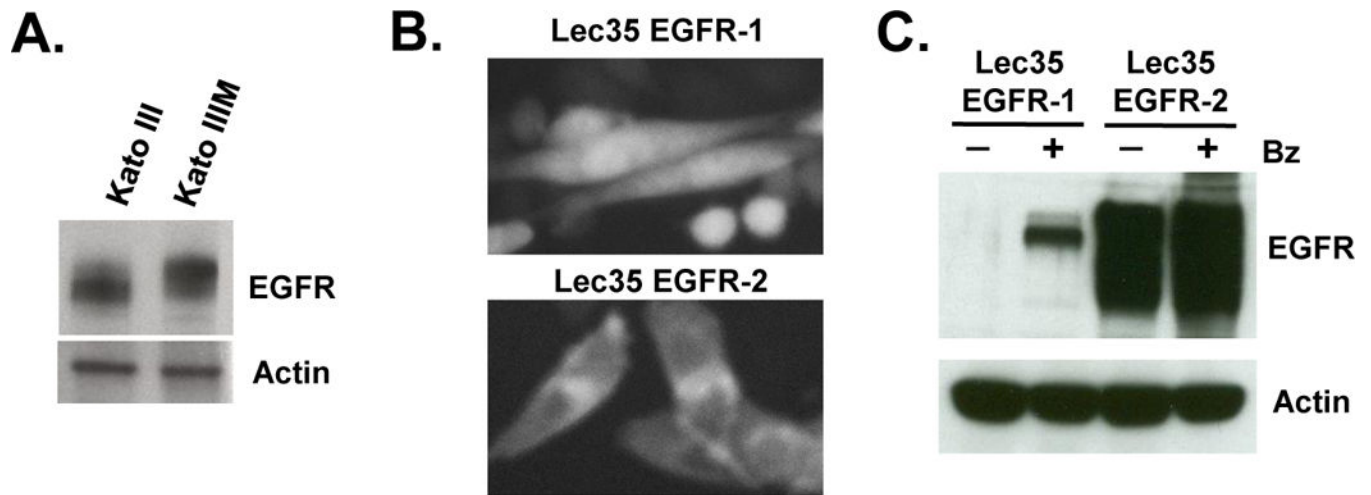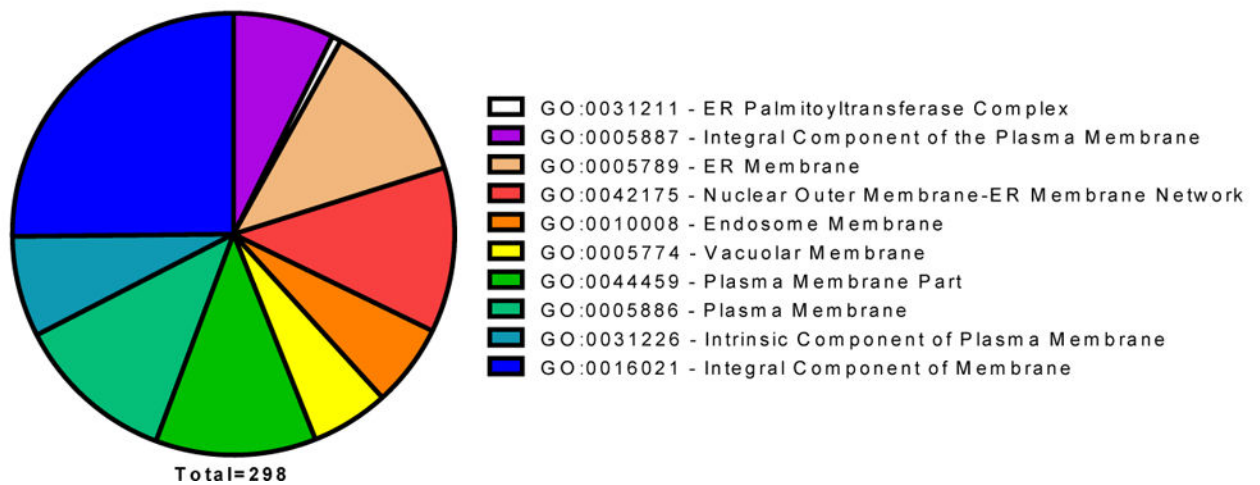
Figure 2. EGFR expression and localization in cells lacking MPDU1

Comparison of EGFR expression and size in KATO III and KATO IIIM by western blot (**A**). EGFR localization (**B**) and expression (**C**) in MPDU1 deficient Lec35 CHO cell clones is shown for comparison. Bortezomib (Bz) treatment was 100nM for 18 hrs.

A.

GO Accession Number	GO Term	Number of Hits	p
GO:0016020	membrane	87	2.39E-04
GO:0044425	membrane part	83	6.14E-07
GO:0031224	intrinsic component of membrane	76	2.56E-06
GO:0016021	integral component of membrane	75	2.78E-06
GO:0044444	cytoplasmic part	64	2.80E-02
GO:0031090	organelle membrane	47	4.56E-09
GO:0044710	single-organism metabolic process	47	3.35E-02
GO:0012505	endomembrane system	44	1.75E-12
GO:0005783	endoplasmic reticulum	37	2.72E-11
GO:0005789	endoplasmic reticulum membrane	36	9.55E-17
GO:0042175	nuclear outer membrane-ER membrane network	36	1.25E-16
GO:0044432	endoplasmic reticulum part	36	1.91E-15
GO:0044459	plasma membrane part	35	1.37E-04

B.

GO:0031211 - ER Palmitoyltransferase Complex
GO:0005887 - Integral Component of the Plasma Membrane
GO:0005789 - ER Membrane
GO:0042175 - Nuclear Outer Membrane-ER Membrane Network
GO:0010008 - Endosome Membrane
GO:0005774 - Vacuolar Membrane
GO:0044459 - Plasma Membrane Part
GO:0005886 - Plasma Membrane
GO:0031226 - Intrinsic Component of Plasma Membrane
GO:0016021 - Integral Component of Membrane

Total=298

Figure 3. MPDU1 rescue induces gene expression changes in Kato III cells

Comparison of Kato III mRNA profiles with those of Kato IIIM. Differentially expressed genes are categorized by gene ontology (GO) term and presented as **(A)** a list of the most enriched GO terms and **(B)** a pie chart of the enriched GO terms.
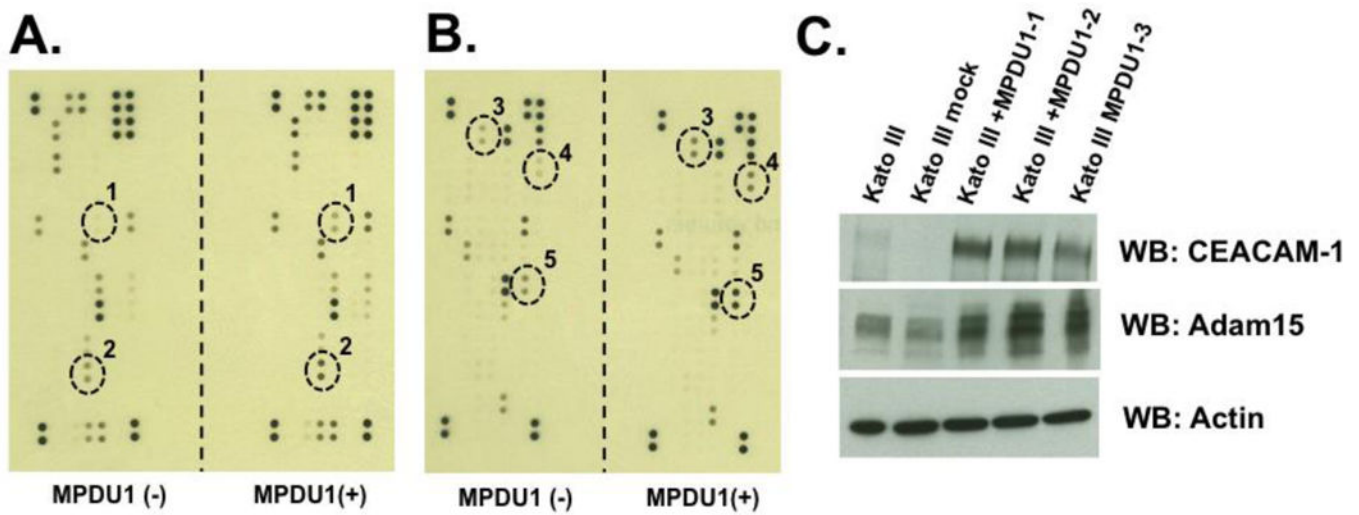
Figure 4. MDPU1 rescue induces protein expression changes in Kato III cells
Comparison of Kato III and Kato IIIM protein expression using the N- terminal **(A)** and C-terminal **(B)** halves of a cell surface receptor array. The levels of five proteins differed between the cell lines: (1) CEACAM-1/CD66a, (2) Integrin B5, (3) Nectin-2/CD112, (4) ADAM15, (5) CEACAM-5/CD66e. **(C)** The changes in CEACAM-1 and ADAM15 levels were confirmed at the protein level by western blotting. Actin was used as a loading control.
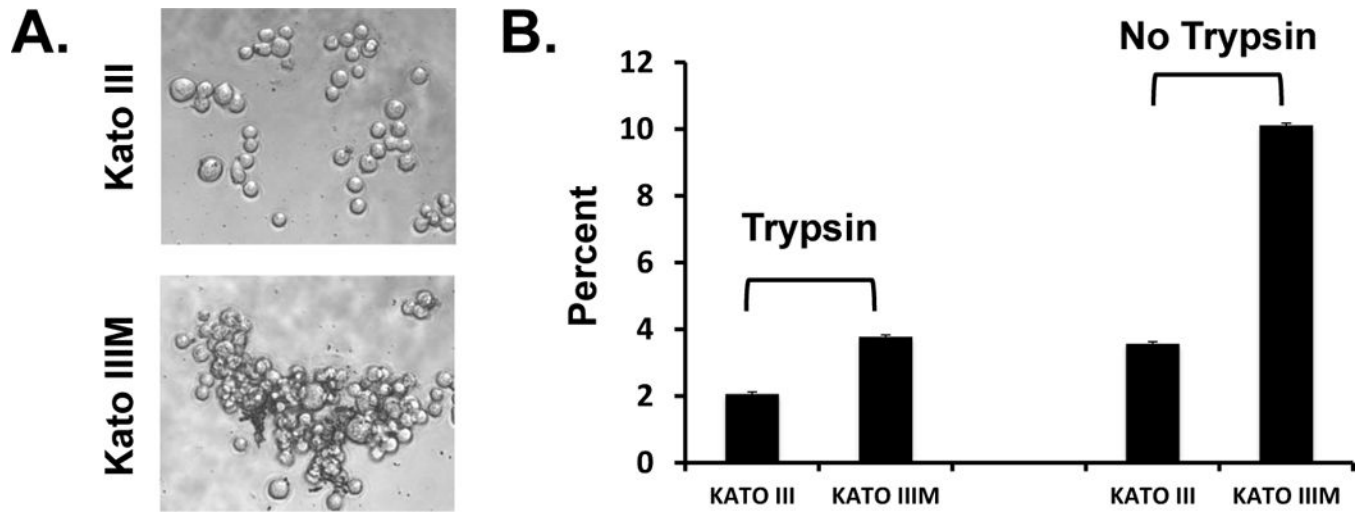
Figure 5. MPDU1 rescue affects cell growth characteristics *in vitro*
In vitro growth of Kato III compared to Kato IIIM using light microscopy **(A)**. Cell aggregation was quantified by measuring size in trypsinized vs non-trypsinized samples **(B.)**. The percent of cell doublet aggregates with size >10 and 20 microns are reported for each condition.
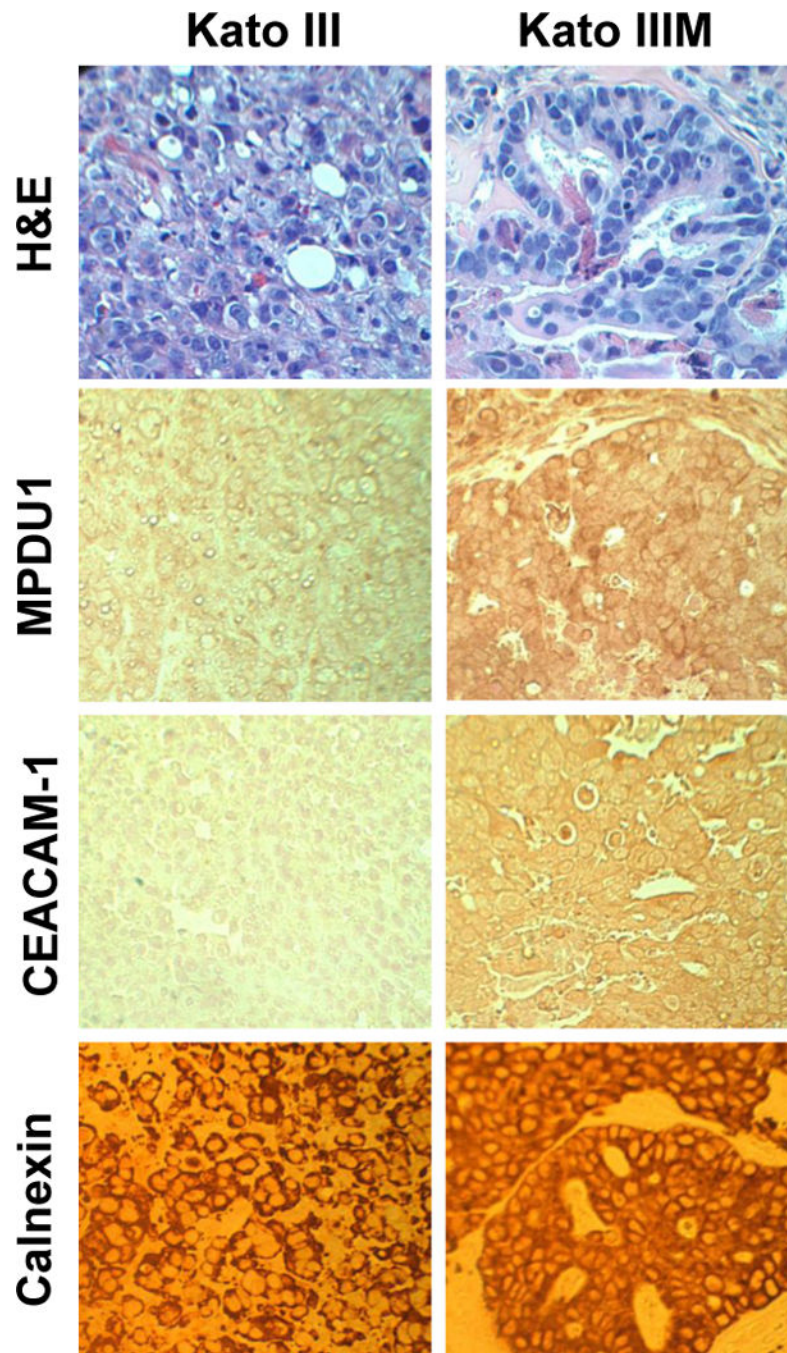
Figure 6. MPDU1 rescue affects cell growth characteristics *in vivo*
Hematoxylin and Eosin (H&E) staining from xenograft tumors demonstrates changes in tumor growth patterns (top panel). Representative IHC of Kato III and Kato IIIM xenografts for CEACAM1, MPDU1, and Calnexin is also shown.

Table 1

***In silico* analysis of N-glycosylation CNVs in cancer cell lines**

Genes involved in NLG were screened for CNVS using the COSMIC cell line project. The number of unique cell lines bearing LOH, amplifications, and deletions is indicated. The asterisk denotes the X chromosome.

Gene	Location	LOH	Amplification	Homozygous Deletion
ALG1	16:5061821-5075588	102	1	0
ALG2	9:101018529-101024067	138	0	0
ALG3	3: 183960089-183967336	60	4	0
ALG5	13:36421967-36471477	188	2	0
ALG6	1:63605886-63675464	67	0	0
ALG8	11:77489636-77528347	81	6	0
ALG9	11:111158129-111247416	127	4	0
ALG10	12:34066483-34072501	112	10	0
ALG11	13:52586555-52586598	189	3	0
ALG12	22:48682862-48698110	165	0	0
ALG13	X:110811069-110890528	342*	0	0
ALG14	1:95220887-95311071	82	5	0
DOLK	9:130747630-130749719	126	0	0
DPAGT1	11:118472424-118477995	124	2	0
DPM1	20:48984811-49008499	35	11	0
DPM2	9:129737199-129740584	127	0	0
DPM3	1:155112438-155112806	43	3	0
MPDU1	17:7427854-7432532	261	0	1
MPI	15:72969450-72977622	89	1	0
PMM2	16:8799193-8850684	88	1	0
RFT1	3:53099851-53139509	210	0	0